

Structural and transport properties of InN grown on GaN by MBE

Kejia (Albert) Wang*, Thomas Kosel, and Debdeep Jena

Electrical Engineering, University of Notre Dame, IN, 46545, USA

Received 14 September 2007, accepted 17 December 2007

Published online 23 April 2008

PACS 61.05.cp, 68.37.Lp, 68.55.-a, 73.61.Ey, 81.05.Ea, 81.15.Hi

* Corresponding author: e-mail: kwang@nd.edu, Phone: + 1-574-6312926, Fax: + 1-574-6314393

In this work, the growth of InN on GaN substrates by molecular beam epitaxy and the structural and electrical characterization are presented. The quality of InN is found to be a sensitive function of the III/V flux ratio and the substrate temperature. The structural quality of InN is characterized by X-ray diffraction, and the transport property is characterized by Hall effect measurements. An optimum growth window to obtain high structural

quality InN with high electron mobility is observed. A strong correlation between the structural quality and the measured Hall mobility is shown. Transmission electron microscope study of InN shows high dislocation density ($\sim 2 \times 10^{11} \text{ cm}^{-2}$ at 200 nm from the InN/GaN interface), which is the limiting factor for the transport property in InN.

© 2008 WILEY-VCH Verlag GmbH & Co. KGaA, Weinheim

1 Introduction Indium Nitride, the least studied semiconductor in the nitride family, has attracted much interest in recent years. Since 2001, high quality InN epitaxial films have been grown by both metal organic chemical vapor deposition (MOCVD) [1] and molecular beam epitaxy (MBE) [2–5]. Optical characterization by photoluminescence shows that the bandgap of InN is around 0.64 eV [6]. Monte Carlo simulation predicts high electron mobility $\sim 10,000 \text{ cm}^2/\text{V}\cdot\text{s}$ and a large saturation velocity of $6 \times 10^7 \text{ cm/s}$ at room temperature [7], which make InN an attractive material for high speed electronic devices. Since the band gaps of the nitride semiconductor family (AlN, GaN, and InN) cover the whole solar spectrum, they are being considered as possible candidates for high efficiency multijunction solar cells, but lattice mismatch problems have to be addressed.

Electrical properties of InN have been studied by Hall-effect measurements. Nominally undoped InN films have shown high electron concentrations ($10^{17} \sim 10^{18} \text{ cm}^{-3}$) [2,5], and electron mobilities exceeding $2000 \text{ cm}^2/\text{V}\cdot\text{s}$ [8,9]. Through a quantitative mobility spectrum analysis (QMSA), a bulk electron mobility of $3570 \text{ cm}^2/\text{V}\cdot\text{s}$ at room temperature has been extracted [10]. The reported electron mobilities are much lower than the theoretical calculation, and it has been pointed out that it

is limited by charged dislocation scattering and ionized impurity scattering [5]. With transmission electron microscopy (TEM), high dislocation densities ($10^9 \sim 10^{11} \text{ cm}^{-2}$) have been observed in InN [11].

In this paper, the growth of InN on GaN substrates using MBE is reported. The effects of III/V flux ratio and substrate temperatures on the crystalline quality of InN have been investigated. The structural property of InN has been studied by X-ray diffraction (XRD) and TEM, and the electron transport properties have been characterized. An optimized growth window is presented to obtain InN with high structural quality and high electron mobility. By comparing XRD characterization results and the electron Hall mobilities, a close relationship between structural and electrical properties has been found.

2 Experimental A Veeco Gen 930 MBE system configured for the growth of III-V nitride semiconductors (InN, GaN, AlN and their alloys) has been used in this work. A UNI-Bulb RF plasma source with an auto-tuner and a network matching controller were used to provide nitrogen radicals. High purity In was evaporated from standard effusion cells. The substrate temperature was controlled by a resistive heater. Commercially available semi-insulating GaN-on sapphire templates were used as

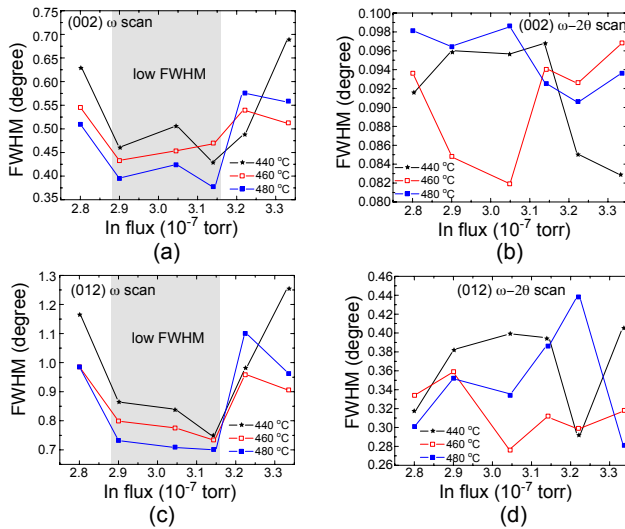


Figure 1 The FWHM of InN peaks in (a) (002) ω scan, (b) (002) $\omega - 2\theta$ scan, (c) (012) ω scan, and (d) (012) $\omega - 2\theta$ scan as a function of In flux at different substrate temperatures.

the substrate. During growth, the nitrogen gas pressure was kept at 2×10^{-5} torr and RF power was fixed at 400 Watt, and the III/V ratio was changed by adjusting the In flux. A 2-step growth process was used: a low substrate temperature (~ 360 °C) InN buffer layer (60 nm) was first grown, followed by a high substrate temperature (440 - 480 °C) epitaxial layer. Three groups of samples grown at 440 °C, 460 °C, and 480 °C respectively were studied. In each group, six samples with In flux (F_{In}) varying from 2.8×10^{-7} torr to 3.34×10^{-7} torr were grown. All 18 samples were grown for 2 hours and had thickness ~ 660 nm. After growth, the samples were examined under an optical microscope. When the In flux was larger than the nitrogen flux, the excess In formed metal droplets visible under the optical microscope after growth. From our study, the crossover boundary between In-rich and N-rich regimes was found to be $F_{In} \sim 3.18 \times 10^{-7}$ torr. After growth, the excess In droplets on the surface were removed by HCl treatment.

To characterize the structural quality of InN films, XRD measurements were taken with a Panalytical X'pert Pro MRD system using the Cu $K\alpha 1$ line. Two types of X-ray measurements were used in this work: rocking curve scan (also known as ω scan) and $\omega - 2\theta$ scan. In the rocking curve scan, the peak is broadened due to the mosaicity, lateral incoherence, dislocations, and sample curvature. In the $\omega - 2\theta$ scan, the peak is broadened due to the lattice constant non-uniformity or strain. Both on-axis (002) and off-axis (012) scans were carried out using rocking curve and $\omega - 2\theta$ scans. The full width at half maximum (FWHM) of the InN peaks for different scanning modes are compared in Fig. 1. From rocking curve scan results in Figs. 1 (a) and (c), InN samples grown at intermediate In fluxes (F_{In} : $2.9 \sim 3.1 \times 10^{-7}$ torr) show smaller

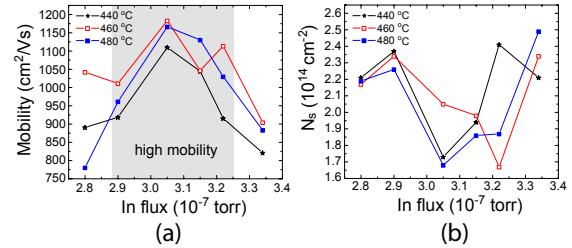


Figure 2 (a) Hall mobilities and (b) sheet carrier concentrations of InN grown on GaN at different growth conditions.

peak broadenings than others, indicating better structural quality. Samples grown at the highest substrate temperature (480 °C) show the best structural quality, followed by samples grown at 460 °C and 440 °C. From Figs. 1 (b) and (d), InN peak broadenings in $\omega - 2\theta$ scan show random distributions and there is no clear trend on how the growth condition affects the lattice constant uniformity. To correlate with investigations of GaN by Heying *et al.* [12], the rocking curve scan results show that InN films grown at intermediate In fluxes (III/V flux ratio slightly smaller than 1) have less threading dislocations.

Room-temperature Hall effect measurements were performed on all the InN samples to study the carrier concentration and transport properties. Van der Pauw technique was employed and Indium dots were used to form ohmic contacts. A magnetic field of 0.3 T was applied and applied dc currents were 1 mA and 0.1 mA. The measured room temperature mobilities and sheet carrier concentrations (N_s) are plotted in Fig. 2. The conductivity of every nominally undoped InN sample was observed to be n-type, and sheet carrier concentrations of all samples are $\sim 2 \times 10^{14}$ cm $^{-2}$. There was no change in carrier densities or mobilities when the Hall measurement was performed in the presence of visible illumination, which can be attributed to the heavy unintentional background doping in InN. The RT electron mobility as high as ~ 1180 cm 2 /V \cdot s is observed. By summarizing XRD and Hall effect measurement results, an optimized growth window for InN is obtained. It is clear that InN films grown at III/V flux ratio ~ 1 and high substrate temperatures (460 \sim 480 °C) have the best structural quality and transport property.

To bring the effect of structural quality on transport properties into a clearer view, Fig. 3 shows the FWHM of the InN X-ray peaks vs Hall mobilities of all InN samples. As seen in Figs. 3 (b) and (d), for the $\omega - 2\theta$ scan, which measures the lattice constant uniformity and strain, the FWHM values show no clear correlation with electron mobilities. So there is no direct correlation between strain and electron mobility in InN. On the other hand, the rocking curve scan can be used to characterize the material structural quality: narrower peak broadenings indicate less defects and better crystalline quality. Heying *et al.* [12] have shown that for wurtzite GaN rocking curve FWHMs (especially off-axis scan) can be used as an indicator of the structural quality such as dislocation density. As seen in

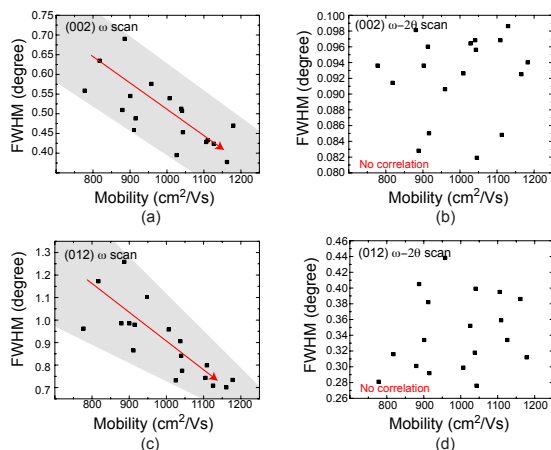


Figure 3 FWHM of InN peaks vs mobilities at (a) (002) ω scan, (b) (012) $\omega - 2\theta$ scan, (c) (012) ω scan, and (d) (012) $\omega - 2\theta$ scan.

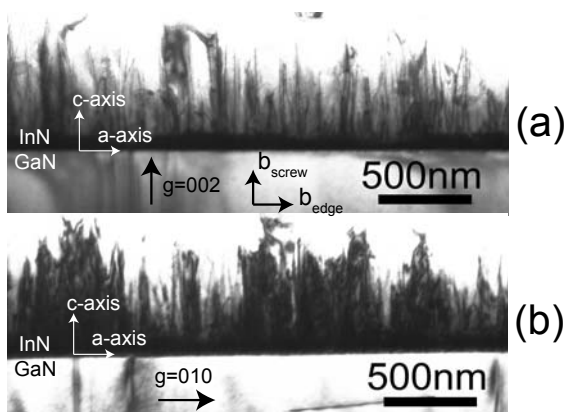


Figure 4 (a) Bright field image of InN at $g=002$. (b) Bright field image of InN at $g=010$.

Figs. 3 (a) and (c), InN with lower FWHM values lead to higher electron mobilities. This observation hints that dislocations are important in determining the nature of electron transport in InN. A high dislocation density broadens the XRD rocking curve scan peak and also results in low electron mobilities due to charged dislocation scattering. Therefore, an investigation of the dislocation density is important.

TEM was carried out using a JEOL 2010 system with 200 kV accelerating voltage to characterize the dislocation density in InN. A cross-sectional TEM specimen was prepared by mechanical wedge polishing and Ar ion milling at 2 keV with liquid nitrogen cooling. Bright field images with $g=002$ and $g=010$ are shown in Figs. 4 (a) and (b) respectively. When the dot product of the g vector and the dislocation Burgers vector is 0 ($g \cdot b = 0$), the dislocation will be out of contrast. With $g=002$ (Fig. 4 (a)), the edge type threading dislocations are out of contrast. The observed threading dislocations are thus of screw type ($b = c$) or mixed ($b = c + a$). With $g=010$ (Fig. 4 (b)), the screw

dislocations with $b = c$ are out of contrast, and edge dislocations and mixed type dislocations will be seen. These dislocations are observed to originate at the InN/GaN interface and propagate towards the surface. At 200 nm from the InN/GaN interface, the density of pure screw dislocation is measured to be about $3.5 \times 10^{10} \text{ cm}^{-2}$, and the total dislocation density is estimated to be about $2 \times 10^{11} \text{ cm}^{-2}$. In an earlier work [5], we have shown that such high dislocation densities result in electron mobilities in the range of $1000 \sim 2000 \text{ cm}^2/\text{V}\cdot\text{s}$, which is much lower than the theoretical predicted $10,000 \text{ cm}^2/\text{V}\cdot\text{s}$ number [7].

3 Conclusion In summary, systematic growth studies of InN grown have been performed. At optimized growth window, InN with good structural quality and high room temperature mobility ($1180 \text{ cm}^2/\text{V}\cdot\text{s}$ for a 660 nm thick InN film), were achieved. By comparing the FWHM of InN peaks in XRD rocking curve scans and Hall effect measurement results, it is found that InN films with smaller FWHM values (better structural quality) lead to higher electron mobilities. Since the XRD peak broadening can be used as an indicator for the total threading dislocation density [12], this result indicates that the charged dislocation scattering is the limiting factor for the transport property in InN. Thus to obtain InN with high electron mobility for high speed device applications, improving the structural quality is of utmost importance.

References

- [1] R. S. Q. Fareed, R. Jain, R. Gaska, M. S. Shur, J. Wu, W. Walukiewicz, and M. A. Khan, *Appl. Phys. Lett.* **84**(11), 1892–1894 (2004).
- [2] H. Lu, W. J. Schaff, J. Hwang, H. Wu, G. Koley, and L. F. Eastman, *Appl. Phys. Lett.* **79**(10), 1489–1491 (2001).
- [3] Y. Nanishi, Y. Saito, and T. Yamaguchi, *Jpn. J. Appl. Phys.* **42**(5A), 2549–2559 (2003).
- [4] C. S. Gallinat, G. Koblmüller, J. S. Brown, S. Bernardis, J. S. Speck, G. D. Chern, E. D. Readinger, H. Shen, and M. Wraback, *Appl. Phys. Lett.* **89**(3), 032109 (2006).
- [5] K. A. Wang, Y. Cao, J. Simon, J. Zhang, A. Mintairov, J. Merz, D. Hall, T. Kosel, and D. Jena, *Appl. Phys. Lett.* **89**(16), 162110 (2006).
- [6] M. Losurdo, M. M. Giangregorio, G. Bruno, T. H. Kim, P. Wu, S. Choi, A. Brown, F. Masia, M. Capizzi, and A. Polimeni, *Appl. Phys. Lett.* **90**(1), 011910 (2007).
- [7] S. K. O’Leary, B. E. Foutz, M. S. Shur, and L. F. Eastman, *Appl. Phys. Lett.* **87**(22), 222103 (2005).
- [8] J. Wu, W. Walukiewicz, W. Shan, K. M. Yu, J. W. A. III, S. X. Li, E. E. Haller, H. Lu, and W. J. Schaff, *J. Appl. Phys.* **94**(7), 4457–4460 (2003).
- [9] G. Koblmüller, C. S. Gallinat, S. Bernardis, J. S. Speck, G. D. Chern, E. D. Readinger, H. Shen, and M. Wraback, *Appl. Phys. Lett.* **89**(7), 071902 (2006).
- [10] T. B. Fehlberg, G. A. Umana-Membreno, B. D. Nener, G. Parish, C. S. Gallinat, G. Koblmüller, S. Rajan, S. Bernardis, and J. S. Speck, *Jpn. J. Appl. Phys.* **45**(41), L1090–L1092 (2006).

- [11] V. Lebedev, V. Cimalla, T. Baumann, O. Ambacher, F.M. Morales, J. G. Lozano, and D. Gonzalez., *J. Appl. Phys.* **100**(9), 094903 (2006).
- [12] B. Heying, X.H. Wu, S. Keller, Y. Li, D. Kapolnek, B. P. Keller, S. P. DenBaars, and J.S. Speck, *Appl. Phys. Lett.* **68**(5), 643–645 (1996).